Stabilized Pulse Spacing in Soliton Lasers Due to Gain Depletion and Recovery

J. Nathan Kutz, B. C. Collings, K. Bergman, and W. H. Knox

***Abstract*— We consider the interpulse dynamics in harmonic passively mode-locked soliton lasers and find that gain depletion in conjunction with its recovery provides an effective repulsion force between adjacent solitons by imparting a group-velocity drift proportional to the interpulse spacings. Analytic descriptions for both the two-pulse and N-pulse per round-trip configurations demonstrate the stability of the equally spaced condition. These theoretical findings, which are supported by experimental results, hold in the limit where cavity losses and perturbations are small per round trip so that the weak gain depletion and recovery mechanisms can dominate the interpulse interactions.**

***Index Terms*— Mode-locked lasers, solitons.**

I. Introduction

CONSIDERABLE interest and research in recent years has focused on developing compact pulsed laser sources with multigigahertz repetition rates for applications in high-speed TDM and WDM communications networks (see [1] and references therein). Since it is difficult to construct a (fiber/bulk) laser cavity which is capable of producing multigigahertz repetition rates in a single pulse per round-trip configuration, efforts have focused primarily on harmonically mode-locked configurations using active modulation techniques [1]–[3]. In particular, lasers mode locked in the anomalous (soliton) dispersion regime tend to produce multiple pulses per round trip since the cavity energy is quantized by the fundamental soliton energy [4], and the total number of pulses in the cavity can be increased by raising the total cavity energy [2]–[7]. This quantization effect is a consequence of increasing the intracavity power and destabilizing the shorter pulsewidth, single pulse per round-trip configuration (which is limited by the gain bandwidth) in favor of multiple pulses per round trip with longer pulsewidths and narrower spectra. Thus, for a high intracavity energy, a given number of propagating solitons will be present. This phenomenon has been predicted and observed by several mode-locking models [8]–[10].

Manuscript received January 26, 1998; revised May 29, 1998. The work of J. N. Kutz was supported by the National Science Foundation University-Industry Postdoctoral Fellowship (DMS-9 508 634). The work of K. Bergman was supported by the National Science Foundation under Grant ECS-9 502 491 and by the Office of Naval Research under Grant N00014-96-0773.

J. N. Kutz is with the Program in Applied and Computational Mathematics, Princeton University, Princeton, NJ 08544 USA, and also with Bell Laboratories, Lucent Technologies and AT&T Research, Murray Hill, NJ 07974 USA.

B. C. Collings and K. Bergman are with the Department of Electrical Engineering and Advanced Technology Center for Photonics and Opto-Electronic Materials, Princeton University, Princeton, NJ 08544 USA.

W. H. Knox is with Bell Laboratories, Lucent Technologies, Holmdel, NJ 07733 USA.

Publisher Item Identifier S 0018-9197(98)06240-X.

When multiple pulses per round trip form in passively mode-locked soliton lasers, the temporal spacings between pulses generally tend to be unstable, and active modulation is frequently employed to maintain equally spaced harmonic operation. However, experimental observations of self-ordering of the pulses into an equally spaced configuration in harmonic passively mode-locked lasers have been reported for both fiber [2], [3], [6] and free-space [5] cavities operating in the soliton regime. Several physical effects, which will be discussed in the following sections, have been proposed to explain the various pulse ordering behaviors. Since it is difficult to apply any single mechanism to the diverse group of experiments on passive harmonically mode-locked lasers, we will focus here on two recent experimental systems that exhibit stable equally spaced (or nearly equally spaced) harmonic mode locking and soliton quantization without the generation of a significant dispersive radiation field [5], [6]. The two lasers considered, a free-space short Cr^{4+}:YAG cavity and a short Er–Yb fiber cavity, are both passively mode-locked with an InGaAs–InP–GaAs–AlGaAs saturable Bragg reflector (SBR) [11]. For these lasers, we propose that the dominant mechanism giving rise to the (nearly) equally spaced multiple-pulse configuration is the interaction of the pulses with the transient depletion and recovery dynamics of the amplifying medium. Thus, the pulses effectively repel each other due to a group-velocity drift caused by the time-dependent gain depletion acting in conjunction with the gain recovery.

This paper is outlined as follows. Section II provides the analytic framework necessary to quantify the effects of the gain depletion and recovery on the temporal spacing of the soliton pulses. In Section III, we explore the interpulse interactions for the 2- and N-pulses per round-trip configurations and show the equally spaced configuration to be asymptotically stable. Section IV provides the details of the experimental setup and highlights the relevant results. We review several other possible mechanisms that may contribute to interpulse dynamics in Section V, and we conclude with a brief summary in Section VI.

II. Governing Equations and Gain Depletion

In a passively mode-locked laser supporting multiple pulses per round trip, an effective mutual repulsion mechanism is required between adjacent solitons in order to achieve (stable) equal spacings between the pulses. In our analysis, we consider the effect of the transient gain depletion and resulting recovery of the laser gain element. Qualitatively, the active ion population inversion of the gain medium is depleted while

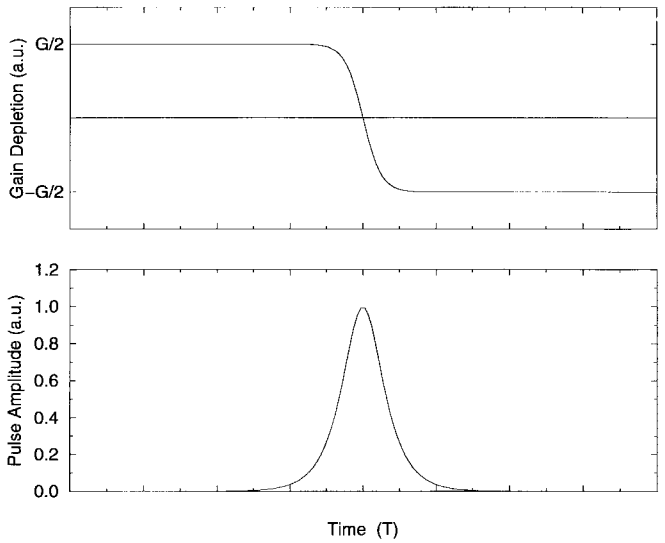

Fig. 1. Qualitative depiction of time-dependent gain across a soliton pulse.

transferring energy to a traversing pulse. Before the next pulse arrives, the population inversion will have a given amount of time to recover before being depleted once again. In the process of depleting the inversion, the pulse experiences a time-dependent gain, i.e., the leading edge of the pulse receives more gain than the trailing edge (see Fig. 1). This time-dependent depletion generates a group-velocity drift of the pulse toward the region of higher gain. The magnitude of this drift is related to the amount of gain given to the pulse and thus to the degree to which the inversion has recovered since the previous pulse.

We begin the analysis by considering the leading order effects to the propagating pulse. Under the influence of the Kerr nonlinearity and group-velocity dispersion (GVD), pulse propagation is described by the nonlinear Schrödinger equation

$$i\frac{\partial Q}{\partial Z}+\frac{1}{2}\frac{\partial^2 Q}{\partial T^2}+|Q|^2Q=0 \tag{1}$$

where Q is the electric field envelope normalized by the fundamental soliton peak field power $|E_0|^2$. The variable T represents the physical time in the rest frame of the mode-locked pulse divided by the factor $T_{\rm pls}/1.76$ where $T_{\rm pls}$ is the full-width half-maximum (FWHM) pulsewidth, and the variable Z represents the physical distance divided by the dispersion period $Z_0=(T_{\rm pls}/1.76)^2/|\beta_2|$ where β_2 is the GVD coefficient. This gives a fundamental soliton peak power of $|E_0|^2=\lambda_0 A_{\rm eff}/2\pi n_2 Z_0$ where n_2 is the nonlinear index coefficient, $A_{\rm eff}$ is the effective cross-sectional area, and λ_0 and c are the optical carrier's free-space wavelength and speed of light, respectively. Note that these soliton scalings are used throughout the remainder of the paper.

In (1), the effects of intrinsic losses, bandwidth limited gain, and intensity-dependent losses have been neglected [8]–[10]. In practice, these terms are generally necessary to describe the mode-locking dynamics which result in the formation of the fundamental solitons observed experimentally [5], [6]. However, once the mode-locked laser achieves equilibrium operation, the resulting fundamental solitons are stabilized by the balance between self-phase modulation (SPM) and GVD. Under these conditions, the loss and gain perturbations can then be effectively neglected [12]–[14] while the mode-locking mechanism can be thought of as a small stabilizing perturbation to the fundamental soliton. We note here that this important simplification may not be valid for laser cavities with significant SPM and GVD per round trip such that the mode-locked pulse is not an averaged soliton of the cavity parameters [5], [9].

Under stable operation, the average gain is driven into saturation until the total gain is equal to the total cavity loss. However, in a mode-locked laser, the gain is not temporally constant. Rather, it is lumped around each propagating soliton pulse. Thus, in considering the spacing of multiple solitons, we introduce a time-dependent dynamical gain perturbation to (1). This perturbation constitutes the mechanism which drives the multiple pulses per round trip toward an equally spaced configuration. We begin by considering the time-dependent depletion of the gain during its interaction with a pulse (see Fig. 1), neglecting any recovery of the gain during this interaction. This is justified since we assume the recovery occurs on a timescale (milliseconds to microseconds) that is long in comparison with the duration of the subpicosecond pulses. We incorporate the transient gain behavior (with its mean value subtracted out) into the pulse propagation equation (1) as a phenomenological perturbation

$$i\frac{\partial Q}{\partial Z}+\frac{1}{2}\frac{\partial^2 Q}{\partial T^2}+|Q|^2Q-i\frac{G}{2}\left(1-2\frac{\displaystyle\int_{-\infty}^{T}|Q|^2dT}{\|Q\|^2}\right)Q=0. \tag{2}$$

Here G measures the magnitude of the depletion which occurs during the pulse interaction. Note that in front of the pulse $(T\to-\infty)$ the gain takes on a value of $G/2$, while behind the pulse $(T\to\infty)$ the gain is $-G/2$ (see Fig. 1). Thus, as the pulse traverses the gain medium, the gain is largest at the leading edge of the pulse and decreases across the pulse as the population inversion is reduced and the gain is depleted. This gain asymmetry causes the pulse to move toward the region of higher gain, i.e., toward $T\to-\infty$. An analytic traveling wave solution exists for (2) which is of the (scaled) form

$$Q=\operatorname{sech}\left[T+\frac{G}{2}Z\right]\exp(iZ/2). \tag{3}$$

This solution explicitly demonstrates the fact that the dynamic depletion response is responsible for a group-velocity drift of the mode-locked pulse toward regions of higher gain. Note that the magnitude of the drift velocity is proportional to the strength of the differential gain response G. This traveling wave solution forms the basis of the equally spaced harmonic mode-locking analysis presented in Section III.

Before proceeding to the next section, we point out that the solution given in (3) is an unstable solution to (2). For instance,

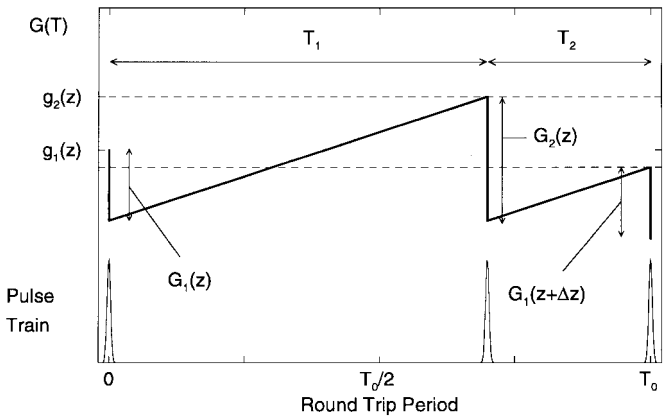

Fig. 2. Qualitative depiction of the time dependent gain with two pulses in the cavity.

dispersive radiation shed for values of $T + GZ/2 < 0$ will experience a net gain due to the differential gain, causing the radiation to grow after many round trips. However, the mode-locking mechanism, which is a much stronger effect than the depletion response, acts to stabilize the pulse by attenuating the low-intensity radiation more than the high-intensity peak of the pulse [9]. Thus, the solution in (3) is effectively stabilized.

III. Interaction Dynamics via Gain Recovery

In this section we incorporate the depletion with the corresponding slow recovery of the gain. In conjunction with the traveling wave solutions found in the previous section, this forms the basis of an analytic description of the interaction dynamics between soliton pulses. The discussion of the interaction is presented in two categories: the two-pulse interaction, for which an explicit solution is found, and the N-pulse interaction $(N > 2)$, for which a linear stability calculation is performed. Both show that an exponentially stable, equally spaced configuration results.

A. Two-Pulse Interaction

We consider a laser cavity with a fixed round-trip time of T_0. The time separating the first and second pulse in the cavity is T_1, while the time separating the second and first is T_2 (note that $T_1 + T_2 = T_0$). Similarly, the strength of the differential gain across the first pulse is G_1 and across the second pulse is G_2. This configuration with the relevant parameters is depicted in Fig. 2.

Since the values of the differential gain G_1 and G_2 determine the drift of each pulse via (3), we consider T_1 and T_2 as a function of distance Z (or round trips). We begin by initially assuming that either $T_1 < T_2$ or $T_1 > T_2$ and consider the relative locations of the pulses as they propagate from a distance Z to $Z + \Delta Z$ where ΔZ is the round-trip distance normalized to soliton units. If initially $T_1 < T_2$, then $G_1 > G_2$ since the gain has a greater amount of time to recover before the first pulse. Thus, the first pulse experiences a larger group-velocity drift (T_1 increases while T_2 decreases). Similarly, if $T_1 > T_2$, then $G_2 > G_1$ so that the second pulse experiences a greater drift relative to the first pulse after a round trip (T_1 decreases while T_2 increases). Here, we assume that the pulses experience the average gain given by the gain medium once per ΔZ. An analytic description is given by the discrete difference equations

$$T_1(Z + \Delta Z) = T_1(Z) + [G_1(Z) - G_2(Z)]\frac{\Delta Z}{2} \quad (4a)$$

$$T_2(Z + \Delta Z) = T_2(Z) - [G_1(Z) - G_2(Z)]\frac{\Delta Z}{2} \quad (4b)$$

where the quantity $(G_1 - G_2)/2$ is the group-velocity difference between the first and second pulses [see (3)].

If we assume that the changes in the pulse and its drift are small per round trip and $\Delta Z \ll 1$, then we can use the definition of derivative to write the continuous versions of (4). In particular, we find

$$\frac{dT_1}{dZ} = \frac{1}{2}(G_1 - G_2)(Z) \quad (5a)$$

$$\frac{dT_2}{dZ} = -\frac{1}{2}(G_1 - G_2)(Z). \quad (5b)$$

By adding and subtracting the system of equations, we find

$$\frac{d}{dZ}(T_1 + T_2) = 0 \quad (6a)$$

$$\frac{d}{dZ}(T_1 - T_2) = (G_1 - G_2)(Z). \quad (6b)$$

The first equation of (6) simply restates $T_1 + T_2 = T_0 =$ constant while the second equation describes the interaction dynamics.

To model the dynamics of the gain recovery, we employ a simple model (summarized by Fig. 2) where we assume the recovery to be linear, a valid approximation if $T_0 \ll \tau$ where τ is the normalized recovery time of the gain medium. Thus, as the first or second pulse encounters the gain medium, a time-dependent depletion of magnitude G_1 or G_2 is experienced by the pulses, respectively. The appropriate recursion relations between the instantaneous gain (prior to interaction with the pulse) of the two pulses is given by g_1 and g_2, respectively

$$g_2(Z) = g_1(Z) - G_1(Z) + \gamma T_1(Z) \quad (7a)$$

$$g_1(Z + \Delta Z) = g_2(Z) - G_2(Z) + \gamma T_2(Z) \quad (7b)$$

and $\gamma = T_0/\tau \ll 1$.

The most basic relationship between the instantaneous gain g_i and the time dependent gain differential G_i assumes that the gain differential is proportional to the instantaneous gain and pulse energy. We assume the laser to be near a steady-state condition such that the variance between the energies of the pulses is small. Thus we take

$$G_i(Z) = \frac{1}{\alpha} g_i(Z) \quad (8)$$

where α is a constant of proportionality which depends upon the pulse energy and magnitude of the total gain. Note that $\alpha \gg 1$ since the magnitude of the gain depletion is small relative to the magnitude of the instantaneous gain. Incorporating this into (7) yields the iterative equations

$$\alpha(G_2(Z) - G_1(Z)) + G_1(Z) = \gamma T_1(Z) \quad (9a)$$

$$\alpha(G_1(Z + \Delta Z) - G_2(Z)) + G_2(Z) = \gamma T_2(Z). \quad (9b)$$

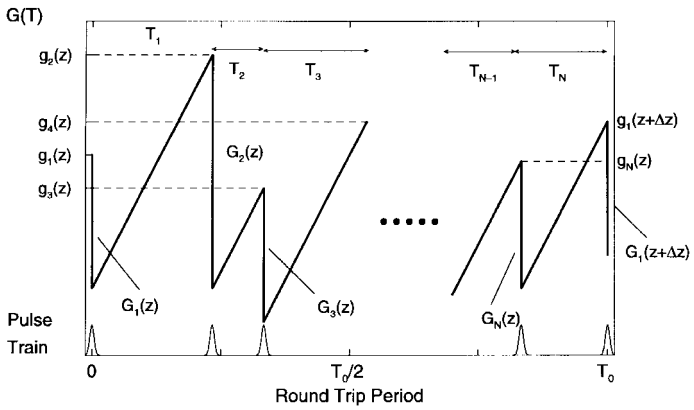

Fig. 3. Qualitative depiction of the time-dependent gain with N pulses in the cavity.

Recall that we require the difference $G_1 - G_2$ evaluated at Z in order to analytically describe the pulse spacing dynamics via (6). Since $\Delta Z \ll 1$, we make use of the Taylor expansion $G_1(Z+\Delta Z) = G_1(Z) + \Delta Z \cdot dG_1(Z)/dZ + \cdots$ in order to subtract and add (9a) and (9b). This yields the approximate system

$$G_1 + G_2 = \gamma(T_1 + T_2) = \gamma T_0 = \text{constant} \tag{10a}$$

$$G_1 - G_2 = -\frac{\gamma}{2\alpha - 1} T_1 - T_2 \tag{10b}$$

where we have dropped $O(\Delta Z)$ corrections since $\Delta Z \ll 1$. Note that the first equation yields the expected result for the case where terms of $O(\Delta Z)$ are neglected and linear decay is assumed, i.e., $G_1 + G_2 =$ constant (see Fig. 2).

Inserting (10b) in (6b) yields

$$\frac{d}{dZ}(T_1 - T_2)(Z) = -\frac{\gamma}{2\alpha - 1}(T_1 - T_2)(Z) \tag{11}$$

whose solution is

$$T_1 - T_2 = (T_1 - T_2)_0 \exp\left(-\frac{\gamma}{2\alpha - 1} Z\right) \tag{12}$$

where $(T_1 - T_2)_0$ is the initial difference between the pulse separation variables.

Thus, as $Z \gg 1$ so that the pulse propagates a large number of cavity round trips, $T_1 - T_2 \to 0$ and we find that

$$T_1 = T_2 = \frac{T_0}{2}, \quad \text{for } Z \to \infty. \tag{13}$$

This suggests that for the case of two pulses in the cavity, the only steady-state (stable) configuration is equally spaced pulses where $T_1 = T_2$ and $G_1 = G_2$. The convergence to this state is exponential with a decay rate proportional to $\gamma/(2\alpha - 1) \approx \gamma/2\alpha$.

B. N-Pulse Interaction

The following analysis provides a general description of the N-pulse interaction case, as shown in Fig. 3. We begin by considering the separation between pulses after each cavity round trip as in the previous section. The analog of (4) for the N-pulse case is

$$T_n(Z + \Delta Z) = T_n(Z) + [G_n(Z) - G_{n+1}(Z)]\frac{\Delta Z}{2} \tag{14}$$

with $n = 1, 2, 3, \cdots, N$ denoting a particular pulse in the pulse train, $G_{N+1} = G_1$, and $T_{N+1} = T_1$. In the continuous limit once again for $\Delta Z \ll 1$, we find

$$\frac{dT_n}{dZ} = \frac{1}{2}(G_n - G_{n+1})(Z) \tag{15}$$

which is the analog to (5).

As before, an appropriate expression for $G_n - G_{n+1}$ is required in order to determine the interaction dynamics. We can simply rewrite the generalized version of (7) which gives

$$g_{n+1}(Z) = g_n(Z) - G_n(Z) + \gamma T_n(Z) \tag{16}$$

with the exception that

$$g_1(Z + \Delta Z) = g_N(Z) - G_N(Z) + \gamma T_N(Z) \tag{17}$$

so that the iterative process is preserved. Here $T_1 + T_2 + \cdots + T_N = T_0$ and (16) and (17) provide the appropriate recursion relation associated with Fig. 3.

Equation (16) does not directly yield an analytic expression for $G_n - G_{n+1}$ as required by (15). However, by once again approximating (17) with the Taylor expansion $g_1(Z + \Delta Z) = g_1(Z) + \Delta Z \cdot dg_1(Z)/dZ + \cdots$ and utilizing (8), we find the relation

$$\alpha(G_{n+1}(Z) - G_n(Z)) + G_n(Z) = \gamma T_n(Z). \tag{18}$$

Since the N degree-of-freedom system (15) with (18) cannot be solved explicitly, we investigate the dynamics with a linear stability calculation about the critical points of (15) [15]

$$G_n = G_{n+1}. \tag{19}$$

From (18), we find that this condition at the critical point implies that $T_n = T_{n+1}$, which then gives

$$T_n = \frac{T_0}{N} \tag{20}$$

at the critical point since $T_1 + T_2 + \cdots + T_N = T_0$.

The stability of this critical point is determined by letting

$$T_n = \frac{T_0}{N} + \tilde{T}_n \tag{21}$$

where $\tilde{T}_n \ll T_0/N$ is a small perturbation to the equally spaced configuration. Inserting this into (18) followed by (15) yields

$$\frac{d\tilde{T}_n}{dZ} = -\frac{\gamma}{2\alpha}\tilde{T}_n \tag{22}$$

whose solution is

$$\tilde{T}_n = \tilde{T}_{n_0} \exp\left(-\frac{\gamma}{2\alpha} Z\right) \tag{23}$$

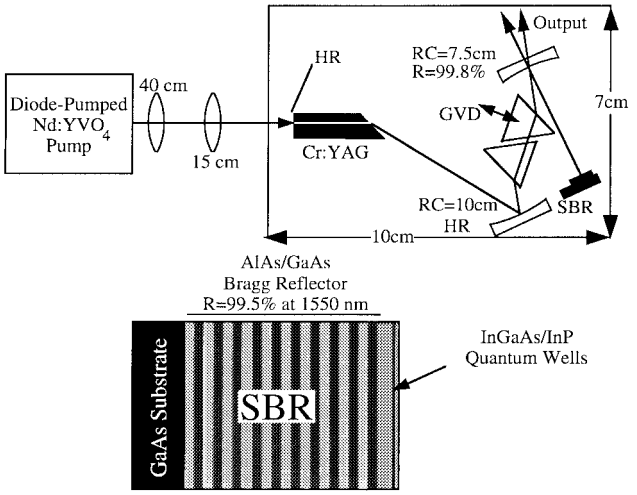

Fig. 4. Schematic of the Cr^{4+}:YAG laser cavity and structure of the SBR. (HR: high reflector; RC: radius of curvature; R: reflectivity).

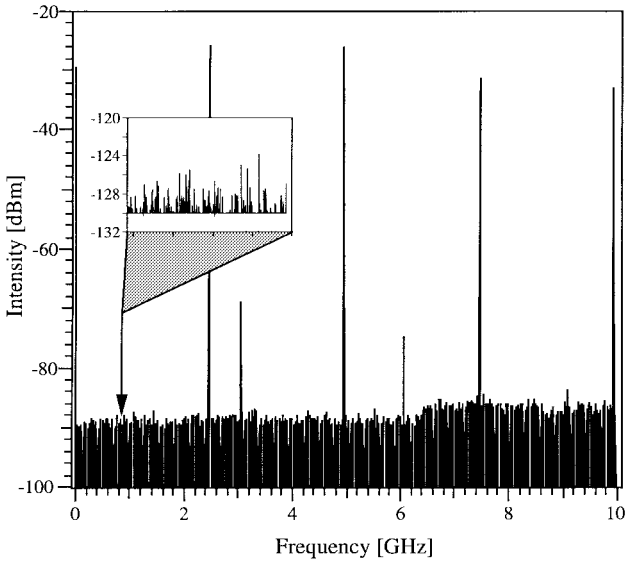

Fig. 5. RF spectrum of the Cr^{4+}:YAG laser output operating with three pulses in the cavity. The inset shows a 4-kHz span with a 1-Hz resolution bandwidth centered about the cavity fundamental frequency illustrating that this component is suppressed by over 110 dB from the harmonic frequency around 2.5 GHz. The tones at 3, 6, and 9 GHz are believed to originate from pump light.

where $\tilde{T}_{n_0}$ is the initial perturbation of $\tilde{T}_n$. Thus, the perturbation $\tilde{T}_n$ decays to zero and the fixed points are exponentially stable, i.e., the equally spaced configuration is achieved. Note that the exponential decay rate $O(\gamma/2\alpha)$ is of the same order of magnitude as that of the two-pulse case. Additionally, achieving equally spaced pulses does not rely on $\Delta Z \ll 1$, i.e., the continuous approximation. Simply solving the difference equations (4) with (7) numerically, it is easy to show that the steady state of the system gives equally spaced pulses.

IV. Experimental Observations

Passive harmonic mode locking is implemented in two different lasers, both of which demonstrate pulse-spacing behavior characteristic of the gain depletion and recovery model. The first is a bulk element solid-state Cr^{4+}:YAG laser and the second is an Er–Yb fiber laser [5]–[7]. Both are passively mode-locked near 1550 nm by a SBR [11] and support multiple fundamental soliton pulses with pulsewidths (FWHM) ranging between 200 and 500 fs. The two laser systems share several characteristic features believed to be essential to the validity of this model: no intracavity active modulation elements are present, the intracavity pulses are solitons of the averaged cavity parameters, and only small perturbations arise from the cavity elements (such as GVD, SPM, gain, and loss).

We begin by considering the short-cavity Cr^{4+}:YAG laser shown in Fig. 4. This 900-MHz fundamental repetition rate cavity consists of a flat/Brewster Cr^{4+}:YAG crystal, a high reflecting focusing mirror, two Brewster prisms, a 0.2% output coupling focusing mirror, and a SBR (also shown in Fig. 4) [5]. The total losses of the cavity are estimated to be ≈1.5%. Passive mode locking is initiated and stabilized by the saturable absorption dynamics of the SBR [16]. From the fluorescence lifetime, the gain recovery timescale (although dependent upon the pumping efficiency) is estimated to be on the order of $\tau = 1\ \mu$s [17]. Furthermore, the interpulse spacing is typically between 0.2–1.0 ns so that the ratio of the gain recovery timescale to the interpulse spacing is approximately $O(10^3) - O(10^4)$.

Due to the fundamental soliton quantization of the total cavity energy [4], passive harmonic mode locking occurs when the total cavity energy exceeds the energy for a single stable fundamental soliton. For this laser, as many as five pulses have been observed to be present. Fig. 5 shows the RF spectrum of the current of a fast photodiode illuminated with the laser output operating with three pulses in the cavity. In this spectrum, the suppression of the cavity fundamentals (multiples of 900 MHz) by over 110 dB indicates that the output pulsetrain is highly periodic, or that the multiple pulses are very nearly equally spaced. Cross-correlating adjacent pulses in the output pulsetrain with a delay of T_0/N measures the relative inter-pulse spacings. Fig. 6(b) shows this measurement for the $N = 3$ case where the multiple pulses are equally spaced (Fig. 6(b) is generated under the same conditions as Fig. 5). Fig. 6(a), an interferometric autocorrelation with the same width as the cross correlation in Fig. 6(b), indicates that the interpulse spacing differs from the ideal value of T_0/N by <20 fs. Fig. 6(c) and (d) show the cross-correlation measurement for the $N = 3$ case where the pulses are not equally spaced. Rather, the interpulse spacings differ from the ideal T_0/N by as much as 4 ps. For all N, we have observed both the equally spaced configuration and the nearly equally spaced configuration for which the interpulse spacings differ from T_0/N by less than 5 ps. Each of these configurations are stable (for several minutes) with external perturbations (i.e., tapping of a mirror) causing the pulses to rearrange into a different steady-state pattern with slightly different temporal spacings.

The Er–Yb fiber laser cavity is shown in Fig. 7 and consists of approximately 16 cm of Er–Yb single-mode fiber ($D \approx -9$ ps/km·nm) and 30 cm of standard telecommunications fiber

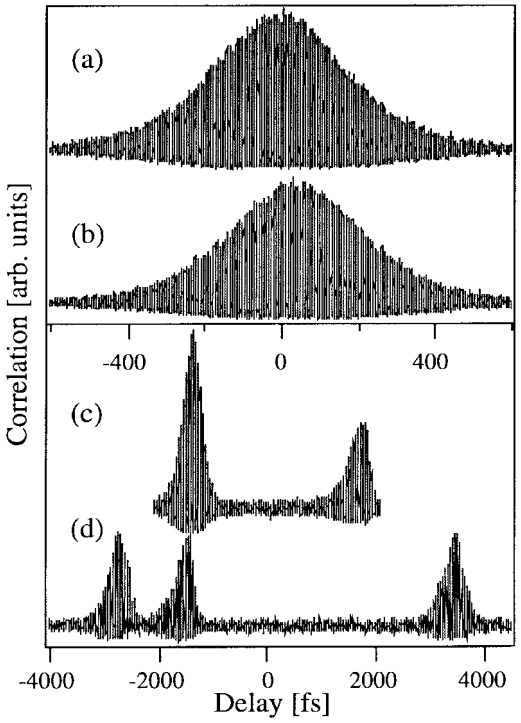

Fig. 6. (a) Autocorrelation and (b)–(d) cross correlations of the Cr^{4+}:YAG laser with three pulses in the cavity. The pulses are equally spaced in (b) and not equally spaced in (c) and (d).

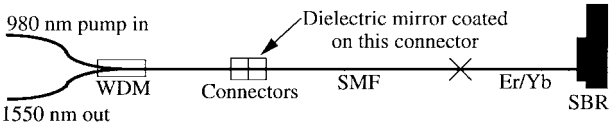

Fig. 7. Schematic of the Er–Yb fiber laser. WDM: wavelength division multiplexer; SMF: single-mode fiber.

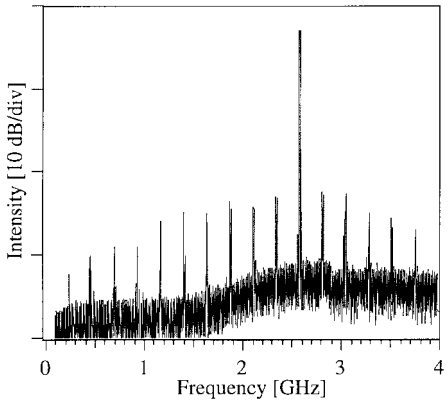

Fig. 8. RF spectrum of the Er–Yb laser output operating with 11 pulses in the cavity.

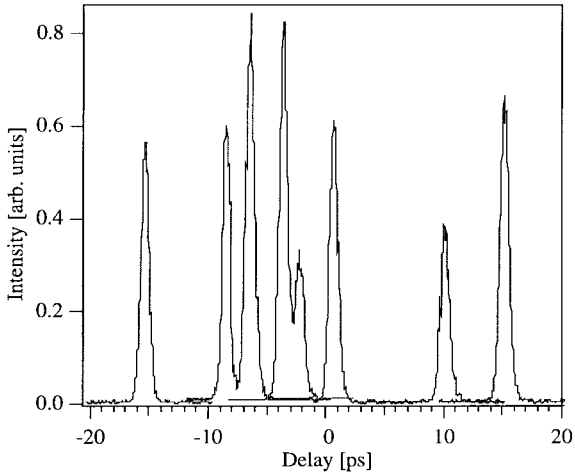

Fig. 9. Cross correlation of the Er–Yb laser output operating with 11 unequally spaced pulses in the cavity.

($D \approx 17$ ps/km·nm) [6], [7]. The SBR is butt-coupled to the cleaved end of the Er–Yb fiber and provides the passive mode locking as in the Cr^{4+}:YAG laser. The unspliced end of the standard fiber is connectorized and coated with a 1.5% dielectric output coupler. For this laser, the gain recovery timescale is estimated to be on the order of 3 ms with the interpulse spacing ranging from ≈0.3 to 1.0 ns. Thus, the recovery to spacing ratio is approximately $O(10^6)$. As in the Cr^{4+}:YAG laser, the total losses are estimated to be ≈2%, resulting in a high finesse cavity. The laser operates with typically up to 11 nearly equally spaced pulses in the ≈250-MHz fundamental repetition rate cavity. Fig. 8 shows the RF spectrum of the current of an illuminated fast photodiode with suppression of the cavity fundamentals by 20 dB. This suppression is typically not observed to be greater than 40 dB. Thus, the strictly equally spaced condition observed in the Cr^{4+}:YAG laser is not observed in the Er–Yb laser. However, as with the Cr^{4+}:YAG laser, the arrangement of nearly equally spaced multiple pulses is stable for several minutes. Fig. 9 shows the cross correlation with $N = 11$, indicating that the interpulse spacing differs from the ideal value of T_0/N by as much as 15 ps.

To summarize these experiments, both equally spaced (within 20 fs) and nearly equally spaced (within 15 ps) multiple pulse harmonic operation occurs in two separate laser systems; one composed of free space elements and the other of fiber. To quantify the error from the strictly equally spaced configuration predicted in the previous section, we divide the maximum difference from the equally spaced configuration by the interpulse spacing. In the Cr^{4+}:YAG laser, this gives an error ranging from ≈0.002% to 2% while in the fiber laser a maximum error of ≈4% is observed. Note that the error is larger for the gain medium with the slower gain recovery time since the depletion and recovery dynamics are more subtle effects.

To make a further connection between experiment and theory, we estimate the predicted timescales required to achieve equal spacing. We first estimate the parameter α in (8) by noting that the absolute gain per round trip must be ≈2% in order to balance the losses. In our normalized units, this gives $g_i \approx 0.02/T_0$. In the two-pulse per round-trip case $G_i = G_1 = G_2 = \gamma T_0/2$ from (10a) so that $\alpha = g_i/G_i = 0.04\tau/T_0$. In the Cr^{4+}:YAG laser, the round-trip cavity time is approximately 1 ns with a gain recovery time of approximately 1 μs. In

this case, $\alpha \approx 40$ and the decay distance required to achieve the equally spaced configuration is $\approx 8\times 10^4 Z_0$, or roughly 0.2–1.1 ms for pulsewidths ranging from 200 to 500 fs. For the fiber laser, the recovery time is $\approx$3 ms with a round-trip cavity time of approximately 3 ns. Thus, equal spacing is achieved in a couple of minutes for the same pulsewidths as in the Cr^{4+}:YAG case. However, in practice, the equally spaced configuration does not occur, rather, the nearly equally spaced configuration is achieved with an error of $\approx$15 ps. These rough estimates are relatively consistent with experiment since the equal pulse spacing in the Cr^{4+}:YAG laser is achieved much faster than is possible to detect with the naked eye (<0.1 s), whereas the fiber laser is observed to require seconds to achieve the equally spaced configuration. The fact that the fiber laser does not exhibit the strictly equal spacing, but rather the nearly equally spaced pulses suggests that the slower relaxation rate (i.e., the gain-recovery perturbation is much smaller and does not dominate as in the Cr^{4+}:YAG) and possibly additional perturbations (as discussed in the next section) play a role in pulse interactions.

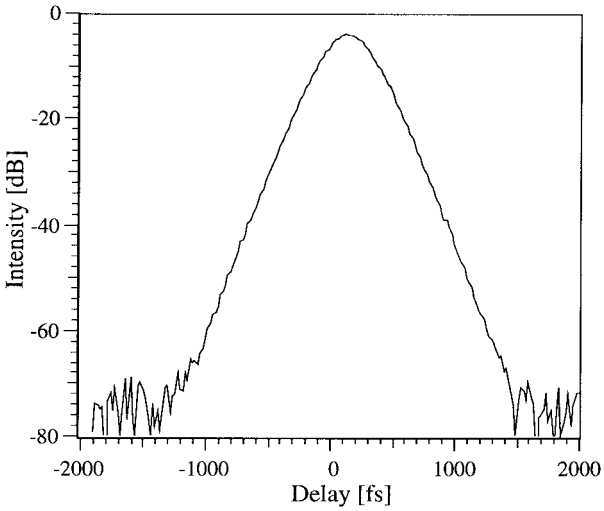

Fig. 10. Plot of the log of the pulse autocorrelation of the Cr^{+}:YAG laser showing the absence of any continuum to $\approx$40 dB.

V. Other Interaction Mechanisms

In this section, we consider a variety of additional mechanisms which have been reported or suggested as interaction mechanisms between pulses in passive harmonically mode-locked lasers. For each mechanism, we will discuss the effect as it pertains to the specific short-cavity weakly perturbed lasers under consideration in this paper. In most lasers, such as bulk solid-state or short-pulse (<100 fs) fiber lasers, the gain and nonlinear and dispersive perturbations are typically larger than in the lasers we are considering here. Although the gain depletion effect will be present, its impact may be negligible in comparison to the larger perturbations so that stable equally spaced pulses are not observed in these lasers.

A. Soliton–Soliton Interactions

It is well known that two fundamental solitons can attract or repel each other depending on their relative phases [18]. Note that this attractive or repulsive mechanism should be distinguished from any interaction which is generated from the dispersive radiation field (as discussed in Section V-B). The soliton–soliton interaction between two pulses, with a relative optical phase of $\pi/2$, will create a repulsion force. In contrast, two solitons which are in-phase will attract. This soliton–soliton interaction fails to explain an odd number of harmonically mode-locked pulses in a cavity since it is not possible to get an odd number of pulses to be mutually repulsive or attractive. Further, if we consider a typical experiment for which the $\approx$300-fs mode-locked pulses are separated by $\approx$100 ps–1 ns, we find that the effective interaction strength between two pulses is of $O(10^{-20})$. This suggests that this effect cannot be the mechanism for equally spaced harmonic mode locking.

B. Soliton-Dispersive Radiation Interactions

The amount of dispersive radiation generated from the quantized fundamental soliton pulses is determined by the cavity [19]. For some long cavities [2] (tens of meters), it is observed that a substantial amount ($\approx$10%) of nonsoliton component (dispersive radiation) can be supported in the cavity [2]. Thus, the dispersive radiation can create an attractive or repulsive force between solitons [2], [20], [21]. However, for the short high-finesse cavities considered here, this nonsoliton component is extremely small. This is clearly seen in Fig. 10 which depicts the log of the pulseshape of the Cr^{4+}:YAG laser and shows that to $\approx$40 dB, there is no continuum evident. This absence of a dispersive radiation field allows for a quantization of solitons which is virtually free of any nonsoliton components [5]. Although this mechanism may play an important role in some cavities [2], we believe it to have little effect on the interaction dynamics for the short cavities considered here.

C. SBR Recovery

The mode-locking element of the lasers considered here is a SBR which exhibits both an ultrafast and slow response [9], [16]. The slow response has a recovery time which has been measured via pump-probe measurements to be $\approx$14 ps. This decay of the real carriers gives rise to a time-dependent loss across the next pulse which interacts with the SBR. This time-dependent loss can induce a drift in the pulse toward the region of the least amount of loss. As with both mechanisms in Sections V-A and V-B, a decay time of $\approx$14 ps generates only an approximate $O(10^{-20})$ perturbation on an adjacent pulse. Thus, the possible interaction due to the SBR recovery is well below the noise level of the cavity and can be ruled out as a possible contributor to the equally spaced harmonic mode locking. In addition, the SBR slow response would create a drift which would tend to bring pulses closer together [9]. Although one might imagine a situation where all the pulses "chase" each other, this situation is unstable to perturbations since if two pulses begin close together, they would tend to interact, attract, and collide. This is not observed in the experiment.

D. Acoustic Effect and Electrostriction

It has recently been suggested by Grudinin *et al.* [22] that the acoustic effect plays a central role in pulse spacing in harmonically mode-locked fiber lasers. The electrostriction from the intense electric field of the pulses distorts the fiber material generating an acoustic wave which is reflected back on the core by the cladding during the propagation of the next pulse [23]. In addition to equal spacing, analytic studies by Grudinin and Gray [2] and Pilipetskii *et al.* [24] show that pulse bunching is also a possible (stable) configuration. The acoustic effect generates a maximal change in the refractive index of the mode-locked pulse stream at a pulse repetition rate of $\approx$500 MHz. This resonant response at 500 MHz frequency is shown by Grudinin and Gray to produce a maximal index changes of $O(10^{-9})$. This response is bigger than the mechanisms suggested in Section V-A–C and is a reasonable candidate for driving the mode-locked pulse train dynamics in fiber lasers. However, the acoustic effect fails to explain the equal spacing in the Cr^{4+}:YAG laser [5]. We note, however, that the effect of the electrostriction itself can alter the local index of refraction. The associated decay from the locally excited index can then interact with the next pulse which transverses the fiber. But this effect is of $O(10^{-9})$ so that it is still much smaller than the proposed gain-recovery mechanism. However, the electrostriction and acoustic effect may play the dominant role as the next largest perturbation to the gain-recovery so that only nearly-equally spaced pulses are achieved. This is currently being investigated as the source of the $<$5% error in the experimental deviations from strictly equally spaced pulses.

Thus, given the above arguments and their corresponding order of magnitudes, we find that the most reasonable mechanism for equal spacing in the soliton lasers considered here is the gain depletion and recovery dynamics considered in this analysis. This mechanism is $O(10^5)$ larger than the acoustic/electrostriction effect which is its strongest competitor.

VI. Conclusions

We have developed an analytic theory describing the equal (or nearly equal) spacing of pulses in harmonic passively mode-locked soliton lasers. The theory shows that the time-dependent depletion of the gain across the soliton pulse causes a group-velocity drift proportional to the spacing between pulses. We have developed an analytic model capturing the effect of the time-dependent gain on the pulses by including a phenomenological perturbation to the nonlinear Schrödinger equation. The model indicates that the only stable configuration for a cavity supporting both two- and *N*-pulses per round trip is when the pulses are equally spaced. This model is supported by experimental observations in both fiber and nonfiber soliton lasers. In particular, we show that the model's predictions are within 5% of the observed experimental phenomena. In addition, we show that for any given initial condition, the equally spaced configuration is reached exponentially fast with a predicted decay rate consistent with experiment. These theoretical results are believed to hold only where cavity perturbations are sufficiently small so as not to overcome the relatively weak effects of the gain depletion and recovery dynamics. We also conclude that the impact of the time-dependent gain upon the soliton lasers considered here is at least five orders of magnitude larger than the other known physical mechanisms.

Acknowledgment

The authors would like to thank S. T. Cundiff, G. T. Harvey, J. P. Gordon, and T. Damen for helpful discussion related to this work.

References

[1] I. N. Duling, III and M. L. Dennis, *Compact Sources of Ultrashort Pulses*. Cambridge, U.K.: Cambridge Univ., 1995.
[2] A. B. Grudinin and S. Gray, "Passive harmonic mode locking in soliton fiber lasers," *J. Opt. Soc. Amer. B*, vol. 14, pp. 144–154, 1997.
[3] M. E. Fermann and J. D. Minelly, "Cladding-pumped passive harmonically mode-locked fiber laser," *Opt. Lett.*, vol. 21, pp. 970–972, 1996.
[4] A. B. Grudinin, D. J. Richardson, and D. N. Payne, "Energy quantization in figure eight fibre laser," *Electron. Lett.*, vol. 28, pp. 1391–1393, 1992.
[5] B. C. Collings, K. Bergman, and W. H. Knox, "True fundamental solitons in a passively modelocked short cavity Cr^{4+}:YAG laser," *Opt. Lett.*, vol. 22, pp. 1098–1100, 1997.
[6] ———, "Stable multigigahertz pulse train formation in a short cavity passively harmonic modelocked Er/Yb fiber laser," *Opt. Lett.*, vol. 23, pp. 123–125, 1998.
[7] B. C. Collings, K. Bergman, S. T. Cundiff, S. Tsuda, J. N. Kutz, J. E. Cunningham, W. Y. Jan, M. Koch, and W. H. Knox, "Short cavity Erbium/Ytterbium fiber lasers modelocked with a saturable Bragg reflector," *J. Select. Topics Quantum Electron.*, vol. 3, pp. 1065–1075, 1997.
[8] H. A. Haus, J. G. Fujimoto, and E. P. Ippen, "Structures for additive pulse mode locking," *J. Opt. Soc. Amer. B*, vol. 8, pp. 2068–2076, 1991.
[9] J. N. Kutz, B. C. Collings, K. Bergman, S. Tsuda, S. T. Cundiff, W. H. Knox, P. Holmes, and M. Weinstein, "Modelocking pulse dynamics in a fiber laser with a saturable Bragg reflector," *J. Opt. Soc. Amer. B*, vol. 14, pp. 2681–2690, 1997.
[10] M. Romagnoli, S. Wabnitz, P. Franco, M. Midrio, L. Bossalini, and F. Fontana, "Role of dispersion in pulse emission from a sliding-frequency fiber laser," *J. Opt. Soc. Amer. B*, vol. 12, pp. 938–944, 1995.
[11] S. Tsuda, W. H. Knox, J. L. Zyskind, J. E. Cunningham, W. Y. Jan, and R. Pathak, in *Conf. on Lasers and Electro-Optics*, Anaheim, CA, 1996, Paper CFD2.
[12] A. Hasegawa and Y. Kodama, "Guiding-center soliton in fibers with periodically varying dispersion," *Opt. Lett.*, vol. 16, pp. 1385–1387, 1991.
[13] J. C. Bronski and J. N. Kutz, "Guiding-center pulse dynamics of nonreturn-to-zero (return-to-zero) communications systems with mean-zero dispersion," *J. Opt. Soc. Amer. B*, vol. 14, pp. 903–911, 1997.
[14] J. C. Bronski and J. N. Kutz, "Asymptotic behavior of the nonlinear Schrödinger equation with rapidly fluctuating, mean-zero dispersion," *Physica D*, vol. 29, pp. 315–329, 1997.
[15] W. E. Boyce and R. C. DiPrima, *Elementary Differential Equations and Boundary Value Problems*. New York: Wiley, 1986, ch. 9.
[16] S. Tsuda, W. H. Knox, E. A. de Souza, W. Y. Jan, and J. E. Cunningham, "Low-loss intracavity AlAs/AlGaAs saturable Bragg reflector for femtosecond modelocking in solid-state lasers," *Opt. Lett.*, vol. 20, pp. 1406–1408, 1995.
[17] G. M. Zverev and A. M. Shestakov, "Tunable near-infrared oxide crystal laser," in *OSA Proc. on Tunable Solid-State Lasers*, 1989, vol. 5, p. 66.
[18] G. P. Agrawal, *Nonlinear Fiber Optics*. San Diego, CA: Academic, 1989, pp. 130–133.
[19] J. P. Gordon, "Dispersive perturbations of solitons of the nonlinear Schrödinger equation," *J. Opt. Soc. Amer. B*, vol. 9, pp. 91–97, 1992.
[20] M. Midrio, M. Romagnoli, S. Wabnitz, and P. Franco, "Relaxation of guiding center solitons in optical fibers," *Opt. Lett.*, vol. 21, pp. 1351–1353, 1996.
[21] M. Romagnoli, L. Socci, I. Cristiani, and P. Franco, "Role of the dispersive wave in soliton dynamics and interactions," in *New Trends in Optical Soliton Transmission Systems*. Dordrecht, The Netherlands: Kluwer, 1998.

[22] A. B. Grudinin, D. J. Richardson, and D. N. Payne, "Passive harmonic mode-locking of a fiber soliton ring laser," *Electron. Lett.*, vol. 29, pp. 1860–1861, 1993.
[23] E. M. Dianov, A. V. Luchnikov, A. N. Pilipetskii, and A. N. Starodumov, "Electrostrictional mechanism of soliton interaction in optical fibers," *Opt. Lett.*, vol. 15, pp. 314–316, 1990.
[24] A. N. Pilipetskii, E. A. Golovchenko, and C. R. Menyuk, "Acoustic effect in passively mode-locked fiber ring laser," *Opt. Lett.*, vol. 20, pp. 907–909, 1995.

J. Nathan Kutz, photograph and biography not available at the time of publication.

B. C. Collings, photograph and biography not available at the time of publication.

K. Bergman, photograph and biography not available at the time of publication.

W. H. Knox, photograph and biography not available at the time of publication.